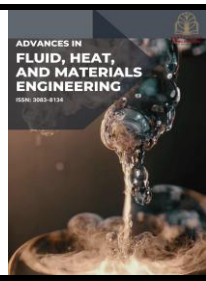




## Advances in Fluid, Heat and Materials Engineering

Journal homepage:  
<https://karyailham.com.my/index.php/afhme/index>  
ISSN: 3083-8134



# Velocity Development in Rectangular Channel with Different Bending Angle

Ahmad Nadzim Jaafar<sup>1\*</sup>

<sup>1</sup> Department of Mechanical Engineering, Faculty of Mechanical Engineering and Manufacturing, Universiti Tun Hussein Onn Malaysia, 86400 Batu Pahat, Johor, Malaysia

---

### ARTICLE INFO

**Article history:**

Received 15 October 2025

Received in revised form 12 December 2025

Accepted 15 December 2025

Available online 21 December 2025

---

### ABSTRACT

This research investigates the study of fluid dynamics in a rectangular channel, focusing on the effect of bend shapes on velocity profiles and flow efficiency. Computational Fluid Dynamic (CFD) simulations of velocity and pressure distributions are carried out in confined flow spaces, with three bend angles 90°, 120°, and 150°. The simulations use a uniform inlet velocity of 10 m/s and the k- $\epsilon$  turbulence model, suitable for high Reynolds number flows, with zero-gauge outlet pressure. This work further explores how boundary conditions, along with turbulence models and flow characteristics, play a role in the development of flow, from uniform velocity to fully developed turbulent flow. The results showed that the increase in bend angle resulted in the stability of flow, reducing the variation in velocity magnitude near the wall. A bigger radius of curvature in 120° and 150° bends reduced flow separation, which caused the uniformity in the velocity distribution. Provide insights for improvements in flow systems in energy-efficient HVAC applications. Maximum velocity comparison shows distinct characteristics of flow, the velocity at 90° is 21.05% higher than 120° and 11.87% higher than 150°, while the velocity at 150° is 8.23% higher than that at 120°. So, the order of magnitude of velocities is as follows, 90° has the maximum value, followed by 150°, and 120° has the minimum value. The analysis further showed that the pressure difference for a 90° bend is 466.2 Pa, exceeding the pressure difference at 120° by 105.7 Pa and that at 150° by 38.9 Pa. Correspondingly, its percentage difference is the highest at 90°, amounting to 279.64%. The pressure difference of 150° outshines 120° by 66.8 Pa, but its percentage difference remains a minimum and amounts to 145.3%. Overall, 90° presented the maximum value of pressure and percentage difference, followed by 150°, and then 120°.

**Keywords:**

Fluid dynamics; CFD simulations; velocity profiles; bend geometry; HVAC systems; angle

## 1. Introduction

Understanding fluid dynamics in rectangular channels has a vital relevance to a wide range of industrial applications, mainly HVAC systems and piping networks. In particular, the development of velocity profiles within these channels plays an important role in optimizing flow efficiency, system design, and energy use in general. For example, velocity distribution in HVAC systems needs to be

---

\* Corresponding author.

E-mail address: dd220052@student.uthm.edu.my

correctly anticipated and regulated to ensure proper air distribution and thermal comfort inside buildings [1,2]. Some of the more basic challenges of designing such systems involve understanding the complex mechanisms that influence flow characteristics, which include separation, recirculation zones [3], pressure losses, and turbulence. The nature of these phenomena is usually very sensitive to geometry and boundary conditions and may change substantially in confined geometries such as a rectangular channel. Flow prediction is a crucial aspect of air supply system design [4], it is for these reasons that computational fluid dynamics (CFD) as a means of analysis has become quite indispensable. CFD simulations can predict velocity and pressure distributions within confined flow spaces and provide insight into the intricate behaviour of fluid flow [5]. CFD simulation methodology cannot be underestimated in this respect, since this is the only method whereby a level of detail can be achieved [5], which practically could not be established by experimental methods alone.

In a rectangular channel, the flow in the channel is subdivided into flow-through regions and recirculation (or stagnation) zones [2]. The dynamics of flow can be influenced by several factors, including Reynolds number, geometry of the channel, and flow conditions that, in turn, may lead to significant changes in the flow behaviour [6-9]. For instance, flow detachment, recirculation zones, and pressure losses commonly occur at bends or blockages along the duct, especially if the turns are sharp or geometries irregular. Such effects lead to a loss in efficiency; hence, their consideration is very essential during the design of fluid flow systems, notably in applications where energy conservation is needed. In order to reduce such losses and enhance the efficiency of flow in HVAC curved channels, a proper understanding of the mechanisms associated with losses is critical [3]. The given work has been designed with an emphasis on the analysis of the velocity profile development from the channel inlet through the outlet, at the same time considering the influence of boundary conditions and turbulence models, particularly the  $k-\epsilon$  model, on the distribution of velocity. The deeper understanding of these very aspects will be rewarding in presenting valuable insight into ways of improving the design and performance of flow systems, particularly within the confined spaces of ventilation ducts and piping networks.

The importance of flow characterization and modelling in ducts is an issue relevant not only to HVAC design but also to many other different industrial applications [1]. An example is the process of aerosol transfer within ventilation systems; the dynamics of the flow, as of the movement of the particles within the air, affect system performance in terms of the health of the individuals subjected to contaminants [10,11]. With HVAC systems, for instance, this will be important in assessing the energy consumed, reducing the noise, and both are very necessary for residential and industrial comfort [11,12]. To capture the complex behaviour of turbulent flows in rectangular ducts, CFD simulations are employed in this study. These simulations allow for a detailed prediction of how the velocity profile evolves under different flow conditions, providing a clearer picture of fluid behaviour [13], pressure variations, and turbulence effects. The study will focus on the  $k-\epsilon$  turbulence model, which has been considered to be well fitted for simulating high Reynolds number flows that are usually noticed within rectangular ducts [14,15]. This model thus captures the main characteristics of turbulence, such as viscosity, kinetic energy, and dissipation-very much essential for the simulation of turbulent flow passing through complex geometries with enhanced accuracy.

The aim of the study is to trace the development of the velocity profile from the inlet to the outlet and investigate the influence of boundary conditions, turbulence models, flow conditions, and various angles on the said development. In particular, the research will be focused on how different angles of bend-90°, 120°, and 150°-will affect the velocity profile in a rectangular channel. It is predicted that the simulations will indicate how the flow is transformed from a uniform inlet velocity to a fully developed turbulent profile by the time it reaches the outlet [16,17]. This will result in the growth of boundary layers near the channel walls, translating to higher velocities at the channel

centreline. The research also explores how the bend geometry, for example, 90°, 120°, and 150°, affects the distribution of flow separation and recirculation zones, especially at the bend and corner areas of the channel. These areas, characterized by acceleration and deceleration of flow, show significant variation in both velocity and pressure. The angle of the bend can augment these variations and might alter flow separation and, consequently, the patterns of velocity and pressure distribution along the channel. The dynamics in such areas are of vital importance since understanding them bestows an enabling capability in the design of more efficient flow systems, particularly those applied in HVAC systems, where stable airflow is essential for proper performance and energy efficiency [18,19]. The close examination of these factors in detail by this study is expected to contribute to the greater understanding of confined flow and the impact of various bend angles on velocity development. It will aid and improve the design and operation of fluid systems in several other industrial applications.

## 2. Methodology

### 2.1 Detail Design of Rectangular Channel

Figure 1 shows the design of a rectangular channel with labeled dimensions in a 3D isometric view. The diagram illustrates the key measurements, including length (L), width (W), height (G), thickness (T), and other structural dimensions, providing a clear representation of the duct's geometry. This image is sourced from a technical drawing, showcasing the typical layout and specifications used in duct design for HVAC systems and industrial applications. The detailed design created with Ansys Fluent's Design Modeler is shown in Figure 1(c). The length of the pipe is within the range dimension indicated in the Ruskin Company catalog [20].

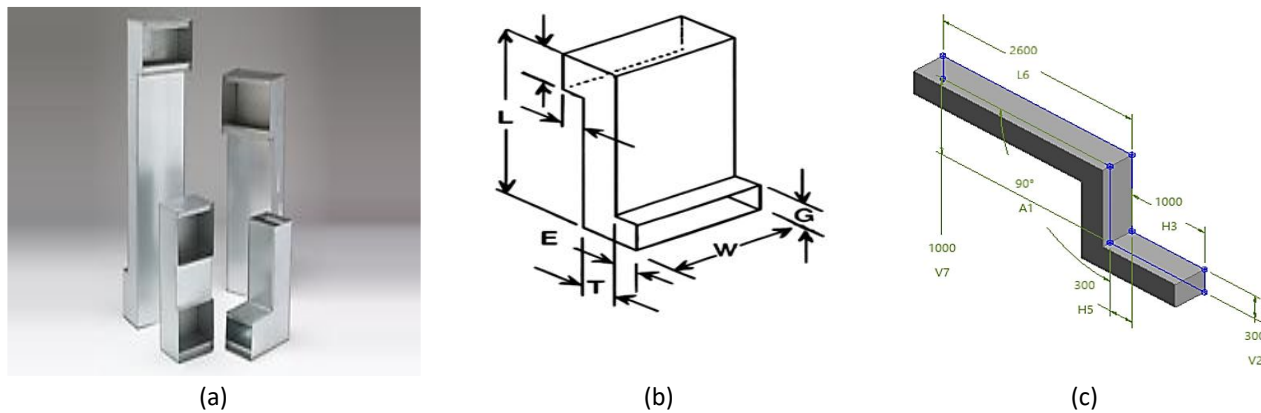


**Fig. 1.** Design of rectangular channel (a) 3D design (b) Technical drawing (c) Design 1

The detailed design of the rectangular channel consists of three configurations with varying bend angles. V1 is the extruded length, acting as the diameter, while V2 is the vertical and H5 is the horizontal width of the channel. The vertical height of the rectangular section is represented by V7, and the inlet length is defined by H3 and L6 is the outlet length of the channel, A1 represents the bend angle, which varies between 90°, 120°, and 150° in the three designs, as shown in Table 1.

**Table 1**

Detail dimension of rectangular channel

Design	V1 (mm)	V2 (mm)	V7 (mm)	H3 (mm)	H5 (mm)	L6 (mm)	A1 (°)
1	400	300	1000	1000	300	2600	90
2	400	300	1000	1000	300	2600	120
3	400	300	1000	1000	300	2600	150

## 2.2 Discretization

The computational domain of the rectangular channel was discretized to enable precise numerical simulation of the flow while retaining computational efficiency. A methodical approach was adopted to generate an outstanding mesh that could capture the complex flow characteristics around the junction. The discretization procedure guarantees that the numerical solution accurately depicts the fluid behaviour inside the channel.

### 2.2.1 Generate mesh

Meshing represents a critical phase in CFD analysis, given that the quality of the mesh directly influences both the accuracy and computational efficiency of the simulation [5]. The mesh generation was performed using the multizone method with mapped type hexa/prism, which is well-suited for capturing the sharp surfaces of the pipe and the geometry of the. Body sizing techniques were applied to control the element size throughout the computational domain.

Figure 2 shows the meshing is designed to discretize the flow domain into smaller elements, enabling computational simulations to solve fluid dynamics equations. Near the walls of the duct, the mesh may be refined to capture the boundary layer effects and the sharp turns in the rectangular channel. This refinement helps improve the accuracy of flow predictions, especially in turbulent regions near the walls and bends. The mesh is crucial for simulating the velocity distribution, pressure drops, and other flow characteristics within the channel.

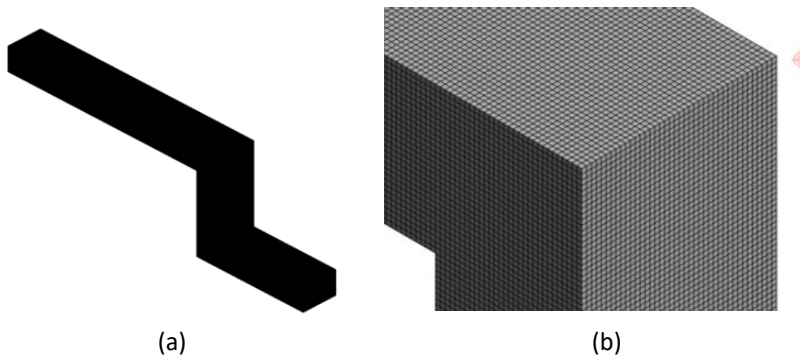


**Fig. 2.** Mesh of fluid domain for Design 1 with element size 8.4 mm  
(a) Isometric view of mesh (b) Detail view of mesh

### 2.2.2 Grid independence test

The grid independence test (GIT) is an important step in computational fluid dynamics (CFD) simulations to make sure that the results are not overly affected by the size or resolution of the grid (mesh). In simple terms, GIT helps confirm that the simulation results are reliable, and that refining the grid further won't lead to big changes in the outcome. This process ensures that the results you get are accurate and can be trusted. By running the test, you essentially check if the grid resolution is fine enough to give meaningful results. If refining the grid (making the mesh smaller) doesn't significantly change the results anymore, you're confident that your solution is stable and accurate. This step is crucial because it helps avoid wasting computational resources on unnecessarily complex grids and ensures the conclusions you draw from the simulation are valid and based on realistic flow behaviour. The truncation error will be computed using Eq. (1) for each mesh configuration.

$$|\frac{A-B}{A}| \times 100 \quad (1)$$

### 2.3 Governing Equation

In CFD, the governing equations are derived from conservation laws. The two-fundamental equations that are used in this analysis are Continuity equation (conservation of mass) and Momentum equation (conservation of momentum) (Navier-Stokes).

#### 2.3.1 Continuity equation (mass conservation)

Eq. (2) represents the principle of mass conservation in fluid flow, stating that the change in density within a small control volume, combined with the net mass flux exiting the volume, must equal zero. Practically, this means that fluid cannot suddenly appear or disappear; whatever enters must either accumulate or flow out. In CFD, the continuity equation ensures that the discretized flow field adheres to this basic physical law, preventing the creation of artificial mass sources or sinks that could otherwise distort the solution, as stated below

$$\frac{\partial \rho}{\partial t} + \nabla \cdot (\rho u) \quad (2)$$

where  $\rho$ = fluid density,  $u$ = velocity vector  $t$ = time.

#### 2.3.2 Momentum equation (Navier-Stokes)

Eq. (3) represents the conservation of momentum by applying Newton's second law to a fluid element. It indicates that the change in momentum (on the left-hand side) results from various forces acting on the fluid, including pressure gradients that push the fluid, viscous stresses that resist motion, and body forces like gravity that add or remove momentum. In CFD, this equation is crucial as it governs how velocity fields evolve under the influence of these forces, capturing how pressure and friction (viscosity) affect flow behaviour, such as acceleration, deceleration, and shear.

$$\rho \left( \frac{\partial \rho}{\partial t} + \nabla \cdot (\rho u) \right) = -\nabla p + \nabla \times \tau + \rho b \quad (3)$$

where  $p$ = pressure,  $\tau$ = viscous stress tensor,  $b$ = body force per unit mass.

### 2.4 Boundary Condition

The boundary conditions for this simulation were set to accurately model velocity development within the rectangular channel. Air was chosen as the working fluid, which is commonly used in piping systems. The inlet velocity was set to 10 m/s [18] to establish a steady, measurable flow entering the domain. Turbulence effects were modelled using the k- $\epsilon$  turbulence model. This model is the most generally [20] for internal flows due to its stability and accuracy in predicting turbulent kinetic energy and dissipation. As for pressure in the outlet, the condition of zero-gauge pressure was applied allowing the fluid to exit freely without any additional pressure constraints. All pipe walls were assigned a no-slip condition, ensuring that the fluid velocity at the wall is zero, reflecting realistic viscous interactions. The solution was initialized using hybrid initialization to generate a physically

reasonable starting field, and the simulation ran for 1000 iterations to achieve convergence and stable flow predictions across the domain.

## 2.5 Velocity Analysis

The analysis of velocity development in the flow via a rectangular channel is important to understand the behavior of fluid while it negotiates regions of confinement, mainly when bends are involved. The velocity profile indicates how well the fluid is flowing and how the geometry of the channel may influence flow dynamics. It is from the study of the distribution of velocity that some regions can be detected where flow separation or turbulence can take place, which causes inefficiency in the system. More precisely, the fluid gains a uniform velocity at its entrance into the channel. However, while negotiating the flow through the bend, such as 90°, 120°, and 150°, the distribution of velocity is different. Considering sharp bends, such as the 90° bend, the flow experiences deceleration along the walls and eventually forms recirculation zones. Such a situation increases energy losses. On the other hand, larger bend angles (120° and 150°) will facilitate the transition of the flow in a smooth way, which reduces the negative effects of separation and consequently enhances the stability of flow. Moreover, the variation of velocity distribution will explain the degree at which different geometries of the bend influence overall flow efficiency, which is vital in application fields, such as HVAC systems, which require steady airflow and minimum loss of energy.

## 2.6 Pressure Analysis

On the other hand, pressure analysis is equally as vital for understanding how the fluid is interacting with the walls of the channel, particularly at bends. The distribution of pressure also corresponds to the velocity profile and reflects the forces acting on the fluid as it flows. By investigating pressure at different bend angles, we can gain insight into where flow is being redirected and where it may meet some resistance. In contrast, in channels with sharp bends, the pressure is significantly higher on the inside of the bend due to the need for acceleration of flow around the curve, whereas on the outer regions, the flow decelerates, which gives rise to a drop in pressure. The variation in pressure can cause inefficient flow, especially when energy consumption is considered. From the analysis of how the variation in the bend geometry influences pressure, it may be possible to devise channel geometries that minimize such pressure drops, and this can lead to more efficient systems. With the increase in bend angle from 90° to 120° and 150°, the distribution of pressure becomes more uniform, indicating that the transition of the flow is smooth. This stability of pressure plays a key role in the reduction of losses and to ensure flow maintains a steady and predictable pattern-a factor that is crucial for the optimal performance of fluid systems in many industrial applications.

## 3. Results

### 3.1 Grid Independence Test (Pressure Drop)

Meshes with varying element size from 8.4-10 mm were executed and the corresponding pressure values were recorded to verify the best element size, as shown in Table 2. The truncation error was computed using Eq. (1) for each mesh configuration listed in Table 2. The mesh with the lowest error, while maintaining an acceptable level of computational efficiency, was chosen for the final simulations, element size of 9.6 mm was selected. This process ensures that the numerical results

accurately represent the physical behaviour of the flow, without being influenced by discretization error.

**Table 2**

Grid independence test (GIT)

Elements size (mm)	Elements	Pressure inlet (m/s)	Pressure outlet (m/s)	Truncation Error (%)
8.4	978236	252.87171	0	-
8.8	849948	230.37291	0	9.766
9.2	748530	247.16850	0	6.795
9.6	657083	254.44618	0	2.860
10.0	583430	237.84089	0	6.981

### 3.2 Velocity Profiles Along the Rectangular Channel

The velocity profiles within rectangular channels at different bend angles  $90^\circ$ ,  $120^\circ$ , and  $150^\circ$  were analysed using computational fluid dynamics (CFD) results obtained from ANSYS Fluent (Figure 3). In the case of the  $90^\circ$  bend, the flow velocity is relatively high at the inlet, but as the fluid approaches the sharp bend, the velocity decreases significantly, especially near the outer walls of the channel. This reduction in velocity is primarily caused by flow separation and the formation of recirculation zones, which are typical in sharp bends. The central region of the channel experiences higher velocities compared to the walls, which indicates the growth of the boundary layer.

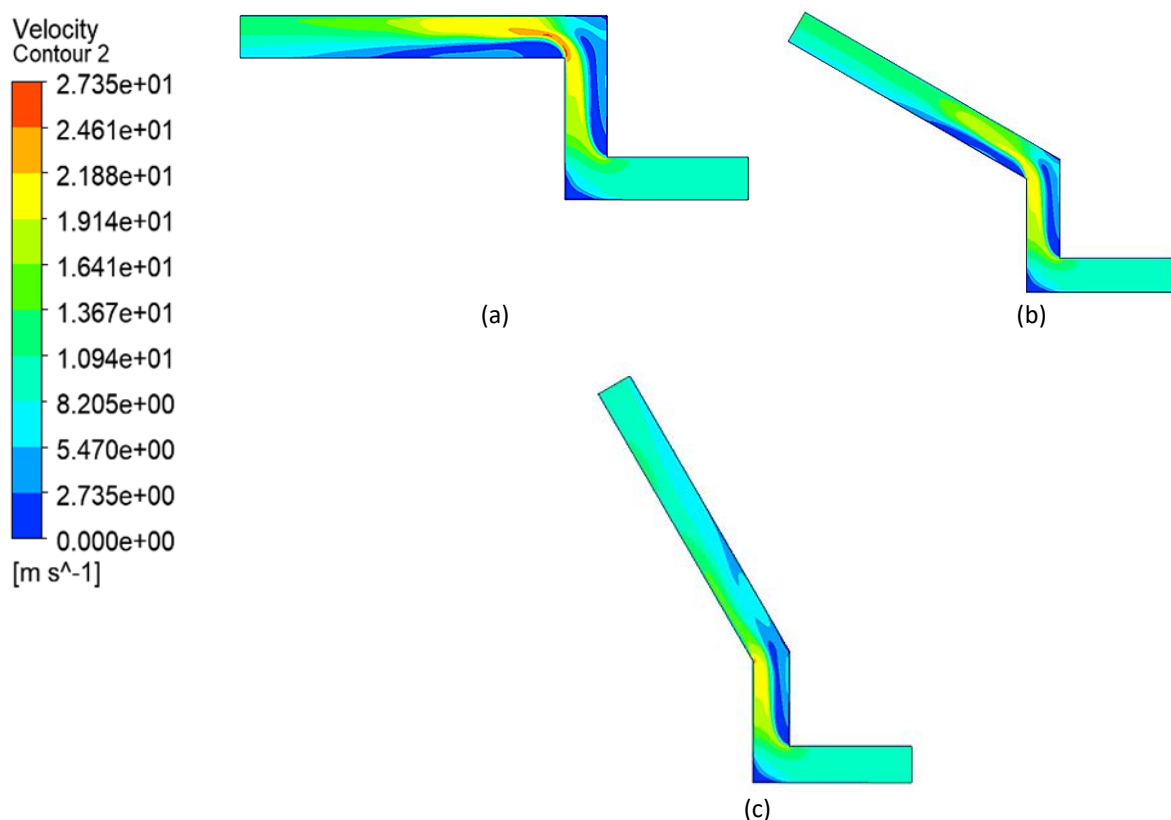


**Fig. 3.** Contour velocity of rectangular channel at different bend angle (a)  $90^\circ$  (b)  $120^\circ$  (c)  $150^\circ$

Subsequently, the velocity contour clearly shows a transition from high velocities (red) at the centreline to lower velocities (blue) near the walls, with the flow accelerating along the centreline and decelerating near the walls due to adverse pressure gradients and separation. With a bend angle

of  $120^\circ$ , the velocity distribution becomes more uniform as the larger bend radius allows the flow to adjust more smoothly to the curvature, resulting in a reduction in the severity of flow separation and recirculation zones compared to the  $90^\circ$  case. Consequently, the reduction in velocity near the outer walls is less pronounced. The velocity contour indicates a wider region with moderate velocity in the centre of the channel, and the flow near the walls experiences less deceleration. The overall velocity profile is more balanced, with a smoother transition between high and low velocities. As the bend angle increases further to  $150^\circ$ , the flow undergoes the least disruption due to the gradual curvature of the channel. The larger bend radius allows for a more cohesive flow, with minimal flow separation or recirculation. The velocity distribution becomes the most uniform of the three cases, with higher velocities maintained near the walls compared to both the  $90^\circ$  and  $120^\circ$  bends. The central region of the channel also exhibits slightly higher velocities, but the flow remains stable throughout the channel.

The contours demonstrate a more consistent velocity profile with reduced variation across the width of the channel. The velocity contour plot provides insight into the velocity distribution, with the colour scale ranging from 0.00 m/s (blue) to 2.735 m/s (red). As the bend angle increases from  $90^\circ$  to  $150^\circ$ , the peak velocity (red) is more centrally located within the channel, and the overall velocity distribution becomes less variable. In the  $90^\circ$  bend, the outer regions of the flow exhibit a significant drop in velocity (blue), whereas in the  $120^\circ$  and  $150^\circ$  bends, the reduction in velocity near the walls is less severe. This indicates that the flow near the walls in the larger bends remains more stable, with less energy loss due to the more gradual turns.

The obtained maximum velocity at the three angles of  $90^\circ$ ,  $120^\circ$ , and  $150^\circ$  show a significant difference in the flow characteristics. At  $90^\circ$ , the maximum velocity is recorded with a value of 27.35 m/s, which is 21.05% higher compared to that at  $120^\circ$  (22.59 m/s) and 11.87% higher than at  $150^\circ$  (24.45 m/s). Moreover, it follows that the velocity magnitude at  $150^\circ$  is 8.23% higher than that at  $120^\circ$ . From the forgoing, it results that the flow at  $90^\circ$  possesses the highest velocity, followed by  $150^\circ$ , while at  $120^\circ$ , this quantity acquires a minimum value. Such an analysis underlines the strong difference in flow intensity among the considered three angles. Consequently, the flow at the angle of  $90^\circ$  is the most dynamic one, whereas at the angle of  $120^\circ$ , the current is less energetic.

### 3.3 Pressure Distribution Along the Rectangular Channel

The analysis of flow through rectangular channels with varying bend angles  $90^\circ$ ,  $120^\circ$ , and  $150^\circ$  was conducted using pressure contour plots to examine pressure distribution across the channel at different angle geometries (Figure 4). In the case of the  $90^\circ$  bend, the pressure distribution reveals a significant pressure increase near the inner bend where the flow is abruptly redirected. The outer bend region experiences relatively lower pressure, creating a noticeable pressure gradient that pushes the flow towards the inner wall. The pressure drops near the inner bend, indicated by blue colouring, reflects the resistance encountered by the flow in making the sharp turn. This sharp contrast in pressure between the inner and outer regions of the bend highlights the effects of the geometry on the flow, with the inner bend showing notably lower pressures compared to the outer bend. Following the  $90^\circ$  bend, the pressure recovers in the outlet section of the channel, with higher pressure values (represented in red) compared to the inlet. In the  $120^\circ$  bend, the pressure distribution is more gradual, with the pressure difference between the inner and outer regions of the bend being less pronounced than in the  $90^\circ$  case, as the flow is more smoothly redirected. While there is still a pressure drop near the bend, the gradient is less severe, and the pressure distribution across the channel becomes more uniform.

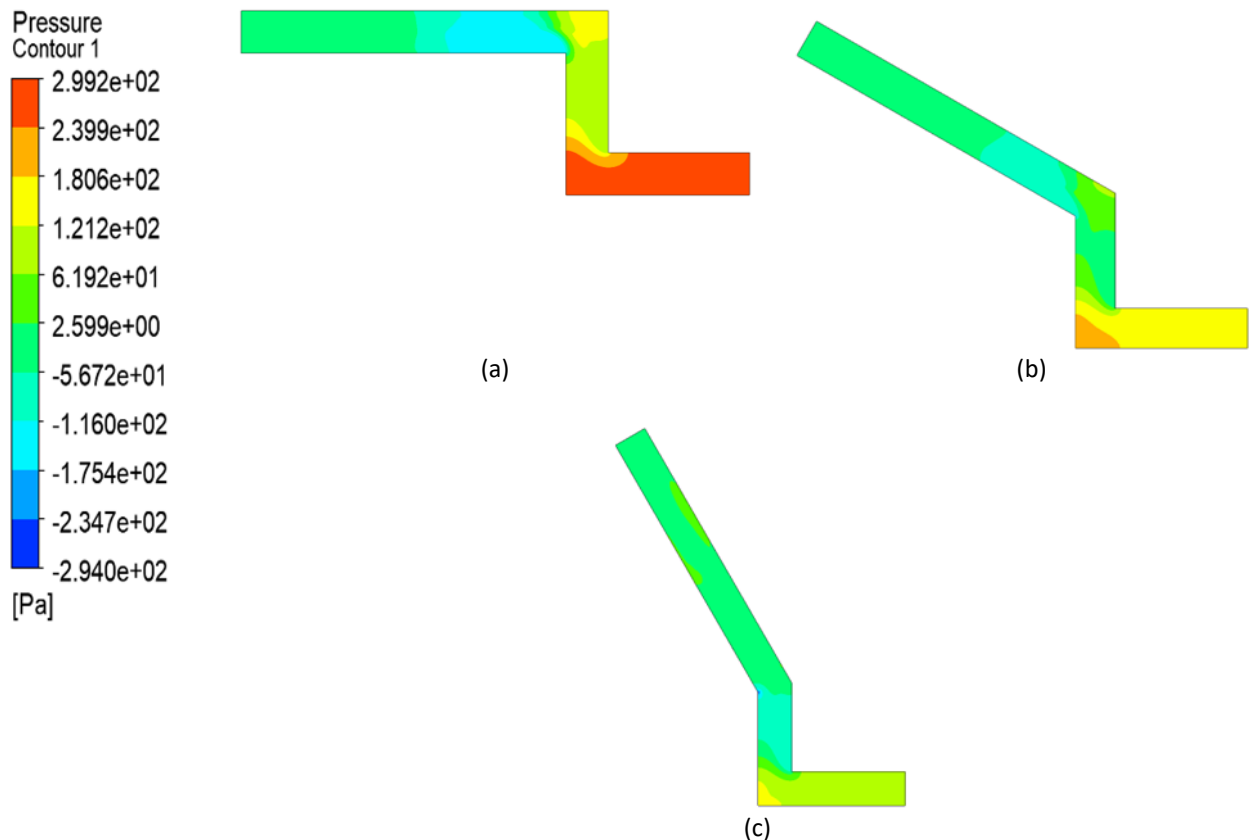


**Fig. 4.** Pressure contour of rectangular channel at different bend angle (a) 90° (b) 120° (c) 150°

The pressure near the inner bend is higher compared to the 90° bend, indicating a smoother flow transition. In the 150° bend, the pressure distribution becomes the most uniform, with a reduced pressure drop near the bend, as the flow undergoes the most gradual turn. The pressure difference between the inner and outer bend is much smaller, resulting in a smoother flow with minimal resistance. The outlet pressure is relatively uniform, reflecting the cohesive flow after the bend. The pressure contour plot further illustrates the range of pressures, from the highest at 2.992e+02 Pa (represented in red) to the lowest at -2.940e+02 Pa (represented in blue), with the inner bend showing lower pressure and the outer bend showing higher pressure. This contour helps visualize the regions where flow separation and recirculation could occur, with the highest pressure at the outlet suggesting a more stable flow following the bend. The results highlight that, as the bend angle increases from 90° to 150°, the flow becomes progressively more stable, with less drastic pressure variations and a more uniform distribution across the channel.

From pressure difference and percentage difference analysis on the three angles 90°, 120°, and 150°, there appear large differences. At 90°, the pressure difference exhibits the maximum value at 466.2 Pa, which surpasses that at 120° by 105.7 Pa (360.5 Pa) and 150° by 38.9 Pa (427.3 Pa). It can thus be suggested that there is a larger pressure difference at 90° as compared with 120° and 150°. Also, as per percentage difference, 90° depicts maximum difference at 279.64%, which depicts 43.79% larger difference as compared with 120° at 235.85%, and 134.34% larger difference as compared with 150° at 145.3%. Conversely, at 150°, pressure difference surpasses that at 120° by 66.8 Pa. However, percentage difference at 150° distinctly reveals lower difference as compared with 90° and 120° at 134.34%, and 90.55%, respectively. It thus implies that 150°, an angle with larger pressure difference as compared with 120°, still depicts smallest percentage difference, suggesting less varying pressure as per compared parameters. Hence, 90° depicts larger pressure difference as well as percent difference as compared with 120° and 150°, and then 150°.

#### 4. Conclusions

The research has effectively explored the effects of bend angles, boundary conditions, and turbulence models on flow dynamics in a rectangular channel. As the bend angle varied from 90° to 150°, it was sighted that there was more uniform velocity with reduced flow disruption and velocity gradients near the walls. Notably, as the bend varied from 90° to 120° and then 150°, there were fewer effects of flow separation and recirculation. From the pressure contour plot, it can be noticed that the pressure profile for a 150° bend is more stable with minimal pressure loss and better-cohesive flow. The result obtained from maximum velocity comparisons showed that velocity at 90° (27.35 m/s) had 21.05% and 11.87% more velocity compared to velocity at 120° (22.59 m/s) and 150° (24.45 m/s), respectively. The result from pressure difference comparisons showed that 90° had a pressure difference of 466.2 Pa, which was 105.7 Pa and 38.9 Pa more compared to 120° and 150°, respectively. Additionally, percentage difference was 279.64%, which showed larger variability. Overall, the study confirms that larger bend angles reduce flow separation and stabilize pressure profiles, improving flow efficiency in rectangular channels. The findings highlight the importance of bend angle, turbulence models, and boundary conditions in optimizing fluid systems for better performance.

#### References

- [1] Malet, Jeanne, Marko Radosavljevic, Modou Mbaye, Delphine Costa, Johann Wiese, and Evelyne Géhin. "Flow characterization of various singularities in a real-scale ventilation network with rectangular ducts." *Building and Environment* 222 (2022): 109223. <https://doi.org/10.1016/j.buildenv.2022.109223>
- [2] Najafi, Amin, and Majid Mesbah. "Understanding pressure loss mechanisms in rectangular air duct elbows: The role of guide vanes." *Journal of Building Engineering* 104 (2025): 112253. <https://doi.org/10.1016/j.jobe.2025.112253>
- [3] Govorukhin, V., and I. Zhdanov. "Steady-state flows of inviscid incompressible fluid and related particle dynamics in rectangular channels." *European Journal of Mechanics-B/Fluids* 67 (2018): 280-290. <https://doi.org/10.1016/j.euromechflu.2017.09.016>
- [4] Ke, Qingdi, Da Fang, Jiwei Sha, and Peipei Cui. "Fluid-structure analysis and prediction of rectangle duct design: a case of air supply system." *Green Manufacturing Open* 2, no. 4 (2024): N-A. <http://dx.doi.org/10.20517/gmo.2024.042901>
- [5] Yuan, Zhitao, Mingliang Zhou, Lixia Li, Zhe Liu, Feifei Liu, Nan Li, and Jiongtian Liu. "Numerical simulation and particle trajectory analysis of knelson centrifugal separation flow field." *Mining, Metallurgy & Exploration* 41, no. 6 (2024): 3563-3580. <https://doi.org/10.1007/s42461-024-01135-7>
- [6] Guo, Pingye, Kai Gao, Meng Wang, Yanwei Wang, and Manchao He. "Numerical investigation on the influence of contact characteristics on nonlinear flow in 3D fracture." *Computers and Geotechnics* 149 (2022): 104863. <https://doi.org/10.1016/j.compgeo.2022.104863>
- [7] Yao, Shuting, Jiansheng Wang, Xueling Liu, and Yu Jiao. "The effects of surface topography and non-uniform wettability on fluid flow and interface slip in rough nanochannel." *Journal of Molecular Liquids* 301 (2020): 112460. <https://doi.org/10.1016/j.molliq.2020.112460>
- [8] Griffith, Boyce E., and Neelesh A. Patankar. "Immersed methods for fluid–structure interaction." *Annual review of fluid mechanics* 52, no. 1 (2020): 421-448. <https://doi.org/10.1146/annurev-fluid-010719-060228>
- [9] Costa, Delphine, Jeanne Malet, and Evelyne Géhin. "An experimental protocol for measuring aerosol deposition In industrial-sized ventilation ducts." *Measurement Science and Technology* 33, no. 9 (2022): 094001. <https://iopscience.iop.org/article/10.1088/1361-6501/ac68d3/meta>
- [10] Miller, Shelly L., William W. Nazaroff, Jose L. Jimenez, Atze Boerstra, Giorgio Buonanno, Stephanie J. Dancer, Jarek Kurnitski, Lindsey C. Marr, Lidia Morawska, and Catherine Noakes. "Transmission of SARS-CoV-2 by inhalation of respiratory aerosol in the Skagit Valley Chorale superspreading event." *Indoor air* 31, no. 2 (2021): 314-323. <https://doi.org/10.1111/ina.12751>
- [11] Ouis, Djamel, Mohammad A. Hassanain, Adel Alshibani, and Ahmed M. Ghaithan. "Noise from heating, ventilation, and air conditioning, HVAC, systems: A review of its characteristics, effects and control." *Journal of Building Engineering* (2025): 113770. <https://doi.org/10.1016/j.jobe.2025.113770>
- [12] Awad, Islam, and Amna Omar. "Noise reduction strategies for heating, ventilation and air-conditioning systems (HVAC)." *Journal of Heritage and Design* 2, no. 7 (2022): 303-314.

- [13] Imran, Muhammad, Kok Keong Lau, Faizan Ahmad, and Afiq Mohd Laziz. "A comprehensive review of Computational Fluid Dynamics (CFD) modelling of membrane gas separation process." *Results in Engineering* 26 (2025): 105531. <https://doi.org/10.1016/j.rineng.2025.105531>
- [14] Miranda, Eduardo P., Daniel Felipe Sempértegui-Tapia, and Cristian A. Chávez. "Turbulence models performance to predict fluid mechanics and heat transfer characteristics of fluids flow in micro-scale channels." *Numerical Heat Transfer, Part A: Applications* 86, no. 13 (2025): 4353-4373. <https://doi.org/10.1080/10407782.2024.2318001>
- [15] Benahmed, Abdelillah, Kaddour Rakrak, Tahar Tayebi, and Mohamed Abdelhak Chohri. "A numerical investigation of the impact of various parameters on the flow and heat transfer in a rectangular duct with inclined obstacles." *Numerical Heat Transfer, Part B: Fundamentals* (2025): 1-14. <https://doi.org/10.1080/10407790.2025.2530676>
- [16] Sharma, Anurag, Bimlesh Kumar, and Giuseppe Oliveto. "Turbulent flow structures in developing and fully developed flows under the impact of downward seepage." *Water* 14, no. 3 (2022): 500. <https://doi.org/10.3390/w14030500>
- [17] Mahananda, M., P. R. Hanmaiahgari, and Ram Balachandar. "On the turbulence characteristics in developed and developing rough narrow open-channel flow." *Journal of Hydro-environment Research* 40 (2022): 17-27. <https://doi.org/10.1016/j.jher.2021.11.003>
- [18] Akeiber, Hussein Jassim. "Computational fluid dynamics modeling of air conditioning systems for energy-efficient buildings." *Al-Rafidain Journal of Engineering Sciences* (2025): 474-504. <https://doi.org/10.61268/v3bw9g08>
- [19] Chowdhury, Ashfaque Ahmed, M. G. Rasul, and M. M. K. Khan. "Thermal performance assessment of a retrofitted building using an integrated energy and computational fluid dynamics (IE-CFD) approach." *Energy Reports* 8 (2022): 709-717. <https://doi.org/10.1016/j.egyr.2022.10.365>
- [20] Stojiljković, Branimir B., and Marta R. Trninić. "An adaptive approach to duct optimization of an industrial boiler air supply system using airfoils." *Thermal Science* 26, no. 3 Part A (2022): 2103-2112. <https://doi.org/10.2298/TSCI210206157S>